Time Resolved EPR of Excited Triplet C_{60} Aligned in Nematic Liquid Crystals†

Stefano Ceola, Lorenzo Franco, and Carlo Corvaja*

Department of Physical Chemistry, University of Padova, via Loredan, 2, 35131 Padova, Italy

Received: July 29, 2003; In Final Form: December 22, 2003

The photoexcited triplet states of fullerenes C_{60} and C_{70} dissolved in a nematic liquid-crystal solvent have been investigated using time-resolved EPR (TR-EPR) spectroscopy. Triplet spectra composed of two lines with opposite polarization (enhanced absorption and emission) and small line widths have been recorded for C_{60}, but much broader lines are recorded for C_{70}. The Jahn−Teller dynamic distortion of C_{60} is responsible for the motional narrowing of the triplet lines, and the partial orientation induced by the nematic solvent removes the degeneracy of the two triplet transitions giving rise to a doublet of lines. Broad features appearing at low temperatures in the nematic phase are attributed to the local disorder induced by the dissipation of excess energy in the photoexcitation process. The time decay of the TR-EPR signals is explained by a kinetic model for the spin-level populations including spin relaxation and selective decay of the spin sublevels.

Introduction

The photoexcited triplet state of C_{60} has been investigated using EPR and ODMR spectroscopy by several groups.[1−8] In a rigid glass matrix, the EPR spectrum extends over about 20 mT, and it shows the typical pattern due to the anisotropy of the electron dipolar interaction. The occurrence of nonvanishing zero-field splitting (ZFS) parameters D and E ($|D| = 12.2$ mT; $|E| = 0.7$ mT) indicates that C_{60} in its triplet state is distorted into a geometry of low symmetry. A static distortion was also observed for triplet C_{60} in the crystalline phase.[9] Moreover, the spectrum is spin polarized with the low-field part in enhanced absorption and the high-field part in emission, as expected from the anisotropy of the ISC process, which selectively populates the zero-field spin sublevels.

In liquid solution, the photoexcited EPR spectrum consists of a very narrow single line, attributed to the excited triplet state.[8] The small line width is not compatible with the rate of molecular tumbling of this rather large molecule. It was accounted for by a fast dynamic Jahn−Teller distortion, which rapidly changes the orientation of the distortion axes with respect to the Zeeman magnetic field.[3] This process corresponds to a pseudorotation of the entire molecule.

Fullerenes are partially oriented when embedded in the nematic phase of a liquid-crystal solvent, as demonstrated by EPR studies of paramagnetic ground-state endohedral fullerenes N@C_{60} and N@C_{70} dissolved in MBBA.[10]

In the present work, we report time-resolved EPR spectra of fullerenes C_{60} dissolved in the liquid-crystal solvent E7. We preferred this liquid crystal, which is nematic over the range of 263−333 K, to other nematic solvents because of its better optical properties, which are more suitable to the investigation of photoexcited states. The EPR of C_{60} in liquid-crystal E7 has already been investigated.[5] The main emphasis was on the dynamics of $^3C_{60}$ in frozen E7. Concerning the temperature range where E7 is nematic, a broad polarized signal was observed, which is attributed to an isotropic distribution of the triplets.

In our investigation, which complements the findings reported earlier, the behavior of C_{60} in the nematic range is studied in more detail. We observed lines that are quite narrow at temperatures close to the nematic−isotropic phase transition. This work focuses in particular on the spin polarization and on the EPR line shape, which are fully described by a simplified dynamical model taking into account the pseudorotation in the presence of the nematic potential.

We have also included the investigation of the C_{70} excited triplet state. In this elongated molecule, the pseudorotation could average only the two axes of the ZFS interaction perpendicular to the elongation axis.[11] This motion should not affect the average orientation of the molecule in the nematic phase.

At the lowest temperatures in the nematic temperature range, the observed spectrum of C_{60} is the superposition of a doublet of narrow lines and a broad spectrum. These features are interpreted on the basis of a superposition of the spectra of the excited-state molecule in two different microscopic environments: disordered and ordered.

Experimental Section

C_{60} and C_{70} were dissolved in toluene at a concentration of about 10^{-4} M. A small amount (0.2 mL) of each solutions was inserted into an EPR quartz tube (3-mm i.d.). Toluene was pumped out under vacuum, and the residual powder was dissolved in the same amount of E7 liquid crystal in the tube. The solutions were degassed with repeated freeze−pump−thaw cycles, and then the tubes were sealed off under vacuum.

TR-EPR measurements were performed by using light pulses to irradiate the sample placed inside the microwave cavity of a X-band EPR spectrometer (Bruker ER200D). A frequency-doubled pulsed Nd:YAG laser was used (Quantel Brilliant: $\lambda = 532$ nm, pulse duration = 5 ns, energy per pulse = 10 mJ). Transient signals were recorded at each magnetic field position. The temperature was controlled by a nitrogen-flow variable-temperature system (Bruker ER4112VT). The TR-EPR signal evoked by the light pulse was amplified by a wide-band preamplifier (bandwidth = 20 Hz−6.5 MHz) and recorded by a digital oscilloscope (LeCroy 344LT). No field modulation was used, and the TR-EPR spectra represent true absorption or

† Part of the special issue "Jack H. Freed Festschrift".

* Corresponding author. E-mail: c.corvaja@chfi.unipd.it. Tel: +39 049 8275684. Fax +39 049 8275135.

10.1021/jp0362178 CCC: $27.50 © 2004 American Chemical Society
Published on Web 03/24/2004

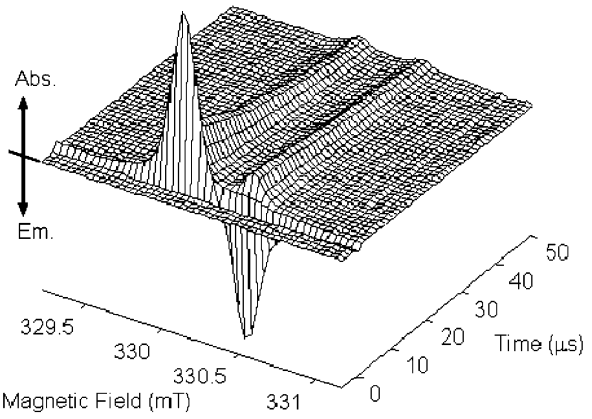

Figure 1. TR-EPR of photoexcited $^3C_{60}$ in liquid-crystal E7 in the nematic phase ($T = 320$ K). Abs. = absorption; Em. = emission.

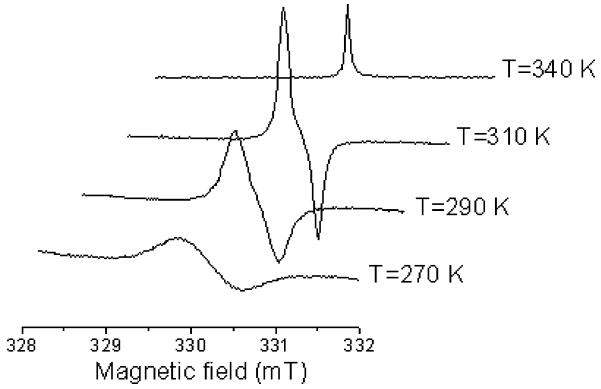

Figure 2. TR-EPR spectra of photoexcited C_{60} in E7 at different temperatures, recorded 0.3 μs after the laser pulse. At 340 K (isotropic phase), the spectrum consists of a single narrow line in absorption. In the nematic phase, the spectrum consists of two lines with opposite polarization.

emission. To increase the signal-to-noise ratio, 100 transient signals were averaged for each magnetic-field value.

Results

C_{60}. A typical TR-EPR signal of photoexcited C_{60} in the nematic phase of E7 is shown in Figure 1 as a function of magnetic field B and time coordinates.

Slices of the surface parallel to the time axis correspond to the average of 100 transient signals as recorded in the experiment at a fixed value of magnetic field B. Slices of the surface parallel to the B axis correspond to EPR spectra at different delays of the laser pulse. Figure 2 shows a series of spectra obtained at different temperatures, recorded at a time delay of 0.3 μs, corresponding to the maximum EPR signal intensity. The spectrum at $T = 340$ K consists of a single narrow line ($\Delta B = 0.03$ mT) centered at $g = 2.0015 \pm 0.0005$.

The line shape and signal time evolution at $T = 340$ K are similar to those observed when triplet C_{60} is generated in toluene solution or in other isotropic solvents.[4,12] The time evolution of this line, shown in Figure 3, is well fit by a double-exponential function such as that shown in eq 1:

$$I = A_1 e^{-t/\tau_1} + A_2 e^{-t/\tau_2} \quad (1)$$

The best-fit values of the exponential time constants (τ_1, τ_2) and the preexponential factors (A_1, A_2) are reported in Table 1. A detailed analysis of the signal evolution will be discussed later.

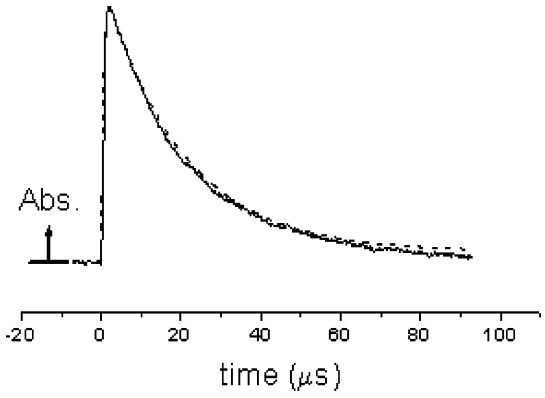

Figure 3. Time evolution of the $^3C_{60}$ EPR signal in the isotropic phase of E7 ($T = 340$ K). The signal was recorded at a magnetic field corresponding to the peak of the single EPR line. (—) Experimental data. (- - -) Double-exponential best-fit function.

TABLE 1: Best-Fit Parameters[a] Obtained Using a Double-Exponential Fitting Function for the TR-EPR Signal of Figure 3, Recorded at $T = 340$ K[b]

parameter	value
A_1	−1.00
τ_1 (μs)	0.53
A_2	+0.74
τ_2 (μs)	19.6

[a] Time constants and normalized preexponential factors. [b] Isotropic phase.

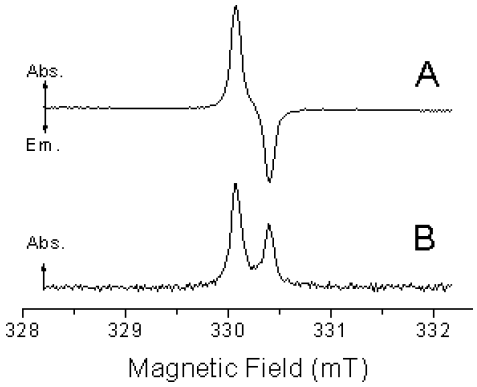

Figure 4. TR-EPR spectra of triplet C_{60} in E7 (nematic phase, $T = 320$ K) taken at different delay times after the laser pulse. (A) 0.3 μs. (B) 15 μs.

The transition from the isotropic to the nematic phase has a dramatic effect on the line shape as shown in Figure 2. The line is split into two components having opposite polarization, the low-field one being in enhanced absorption and the high-field one being in emission. The polarization decays quickly, and about 5 μs after the laser pulse, both lines occur in absorption, though with different intensities as shown in Figure 4.

As the temperature decreases, the line separation increases as shown in Figure 2. At temperatures lower than 285 K, two components are still detectable at short delays when they are spin polarized with opposite phases, but they are not resolved at later times when both are in absorption because of the large line width.

Figure 5 shows the line separation (splitting) as a function of the reduced temperature T/T_{NI}, where T_{NI} is the nematic/isotropic transition temperature.

The splittings reported in Figure 5 have been obtained by fitting with two Lorentzian functions the TR-EPR spectra taken at long delay after the light pulse (15 μs) in order to avoid the

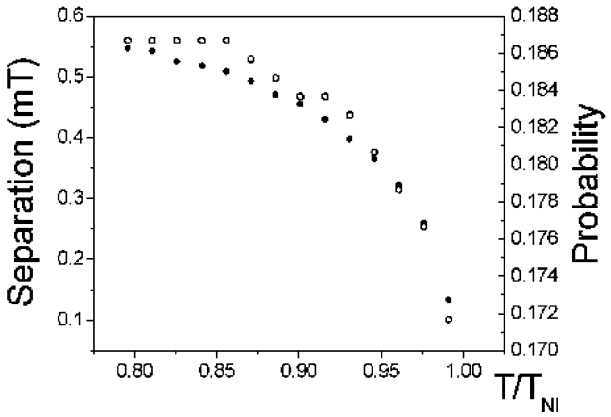

Figure 5. (○) Triplet C_{60} EPR line splitting; (■) probability of the $\theta = 0°$ site (B_0 parallel to the z axis of the triplet tensor) measured in the nematic phase as a function of the reduced temperature T/T_{NI}. T_{NI} is the nematic−isotropic transition temperature.

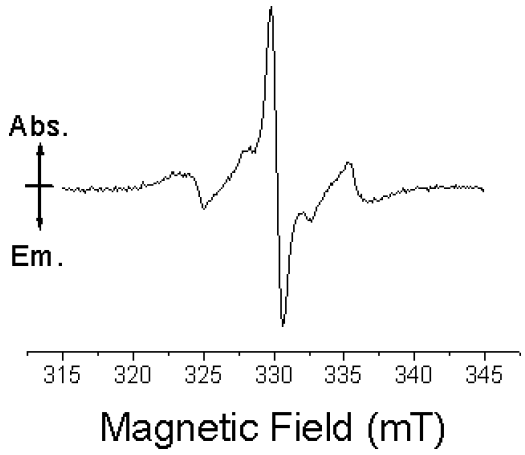

Figure 6. TR-EPR spectrum of $^3C_{60}$ at $T = 280$ K taken 0.3 μs after the laser pulse. In addition to the two narrow lines shown at higher temperatures, additional features are displayed with much larger spectral width.

spectral distortions occurring at short time delays, in particular, those at low temperatures. In fact, by decreasing the temperature (from 290 down to 263 K, which corresponds to the nematic/soft-glass transition temperature), additional features appear at the wings of the spectrum, as shown in Figure 6. They decay much faster than the narrow doublet in the center of the spectrum.

The time evolution of the signals taken at the magnetic fields corresponding to the maximum absorption and emission intensities of the narrow doublet is shown in Figure 7.

The decay of the signals is described by a sum of two exponential functions, whose time constants and relative weights are collected in Table 2.

TABLE 2: Best-Fit Parameters[a] Obtained Using a Double-Exponential Fitting Function for the TR-EPR Signals of Figure 7, Recorded at $T = 320$ K[b]

	low-field line (absorption)	high-field line (emission)
A_1	0.1	0.04
τ_1 (μs)	18.6	40.5
A_2	0.8	−1.0
τ_2 (μs)	0.32	0.41

[a] Time constants and normalized preexponential factors. [b] Nematic phase.

C_{70}. The TR-EPR spectrum of photoexcited triplet C_{70} in the nematic phase of E7 is quite different from that measured for C_{60}. At a short delay after the light pulse, it consists of broad features extending over a magnetic-field range of 20 mT. The polarization pattern is the same as for C_{60} with the low-field half of the spectrum in enhanced absorption and the high-field one in emission, as shown in Figure 8A.

The spectrum has the same spectral width and the same polarization pattern as that obtained in isotropic glassy solvent as toluene at low temperature.[11]

The spectral shape changes at longer delay times after the laser pulse because of the different temporal behavior of the spectral components, and the line width decreases dramatically. At times longer than 4 μs from the light pulse, a broad single line in absorption is observed, characterized by a Lorentzian shape and a width of $\Delta B = 3.7$ mT as shown in Figure 8B. In liquid toluene at 290 K, a single line is recorded with $\Delta B = 1.27$ mT.

Discussion

EPR in Partially Oriented Solvents. The EPR spectrum of photoexcited C_{60} and of C_{70} in glassy solution is accounted for by the following spin Hamiltonian:

$$H = g\beta \mathbf{B}S + \mathbf{D}\left(S_z^2 - \frac{1}{3}S^2\right) + E(S_x^2 - S_y^2) \qquad (2)$$

In terms of the principal values (X, Y, and Z) of the electron dipolar interaction tensor **D**, the zero-field parameters D and E are defined as $D = -(3/2)Z$ and $E = (1/2)(Y - X)$. For C_{60} and C_{70}, parameters D and E and the ratios of the populating rates of the zero-field spin sublevels are reported in several papers.[6,7] The values are collected in Table 3. The sign of D is considered to be negative for C_{60} and positive for C_{70}.[13,14]

In anisotropic solvents such as liquid crystals, each molecule experiences all orientations with differing probabilities. For fast molecular motion, the ZFS tensor is averaged over the orientation distribution, giving an effective ZFS tensor having axial symmetry around the liquid-crystal director. The effective ZFS

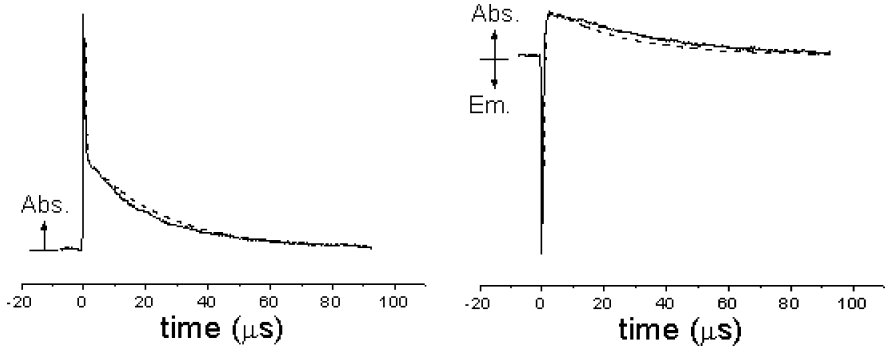

Figure 7. Time evolution of the low-field line (left) and high-field line (right) of triplet C_{60} in the nematic phase ($T = 320$ K).

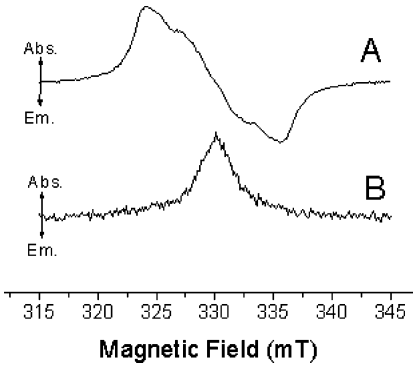

Figure 8. TR-EPR spectra of triplet C_{70} in E7 (nematic phase, $T = 320$ K) taken at different delay times after the laser pulse. (A) 0.3 μs. (B) 4 μs.

TABLE 3: ZFS Parameter Values and Population Ratios for the Triplet States of C_{60} and C_{70} as Reported in the Literature

	D (mT)	E (mT)	$P_x/P_y/P_z$
C_{60}[a]	−12.2	+0.6	1:1:0
C_{70}[b]	+5.3	−0.6	0:0:1

[a] Reference 6. [b] Reference 7.

parameter (D_{eff}) is obtained from the ordering matrix **S** and the ZFS tensor **D**.[15,16]

$$D_{\text{eff}} = -\text{Tr}[\mathbf{S}\cdot\mathbf{D}] \tag{3}$$

The director of nematic liquid crystals is oriented by a magnetic field, and the EPR spectrum of a triplet-state molecule dissolved in these solvents consists of two lines whose separation is $2D_{\text{eff}}$. This parameter depends on the temperature because of the temperature variation of the ordering matrix **S**.

The shape of the spectrum of photoexcited triplet states depends on the relative populations of the triplet sublevels P_{-1}, P_0, and P_1, which at short delay time after a laser pulse are proportional to the populating rates k_r. It is usual to define **P** as a diagonal matrix with elements proportional to k_r. The population difference between the triplet sublevels ($\Delta P_{\pm}$) also depends on the relative orientation between the molecular frame and the magnetic-field direction. This is given by

$$\Delta P_{\pm}(\Omega) = \pm \sum_{m=0,\pm 2} a_m D^2_{0m}(\Omega) \tag{4}$$

where D^2_{0m} represents the second-rank spherical harmonics, $\Omega = (\alpha, \beta, \gamma)$ represents the three Euler angles of the molecular frame with respect to the magnetic-field direction, and a_m represents the irreducible spherical components of matrix **P**.

If the motion is sufficiently fast, then the angular dependence is averaged over the proper orientational distribution function. The population difference becomes

$$\Delta P_{\pm} = \pm \sum_{m=0,\pm 2} a_m \overline{D^2_{0m}} \tag{5}$$

where the upper bar over the spherical harmonics stands for the integration over Ω. $\overline{D^2_{0m}}$ represents the spherical components of the ordering matrix **S**.

$$S_{zz} = \overline{D^2_{00}} \tag{6a}$$

$$S_{xx} - S_{yy} = \sqrt{\frac{3}{2}}(\overline{D^2_{0+2}} + \overline{D^2_{0-2}}) \tag{6b}$$

$$a_0 = P_x + P_y - 2P_z \tag{7a}$$

$$a_{\pm 2} = \frac{P_y - P_x}{2} \tag{7b}$$

Because of the uniaxial character of the nematic phase, $S_{xx} = S_{yy} = -2S_{zz}$ and both D_{eff} and $\Delta P_{\pm}$ depend on a single order parameter S. With some algebra, the following expression is obtained:

$$\Delta P_{\pm} = \pm\text{Tr}[S\cdot P] \tag{8}$$

EPR Line Shape. Mehring et al. performed computer simulations of the spectra of triplet C_{60} in frozen toluene (at different temperatures) using several models, and they concluded that a jumping process takes place between 12 sites.[17] These correspond to the D_{5d} axially distorted structures of C_{60}.[18] The jumping process is slowed by lowering the temperature, becoming frozen only at very low temperature. The rotational diffusion dynamics was studied by Levanon et al.[19]

The spectrum recorded in the nematic phase consists of two narrow lines. This is due to a fast motional averaging of dipolar splitting, assuming an anisotropic distribution of the solute molecule. The detection of a partial alignment of C_{60} completes previous findings reported in ref 5.

Because the solvent is partially oriented along the Zeeman magnetic field B, the electron dipolar interaction is not completely averaged to zero, and the degeneracy of the $T_{-1} \leftrightarrow T_0$ and $T_0 \leftrightarrow T_1$ EPR transitions is removed. However, at least close to the nematic−isotropic transition temperature, the line width does not show remarkable variation, and it remains unusually small for a triplet state in solution. For this reason, we suggest that the line-narrowing process due to the dynamic Jahn−Teller effect is still operative. In the nematic phase, the distortion occurs in the presence of a nonisotropic potential, and the directions of distortion are not isotropically distributed.

We discuss the line splitting and polarization features of triplet C_{60} in E7 on the basis of the following assumptions:

(1) $D < 0$[14] and the zero-field sublevel populating rates in nematic E7 are the same as in the low-temperature glass phase ($P_x/P_y/P_z = 1:1:0$).

(2) The molecule is distorted along a C_5 symmetry axis,[20] and the z principal axis of the electron dipolar interaction coincides with C_5.

(3) The rhombic distortion is negligible ($E = 0$). This condition justifies the assumption of equal populating rates of the x and y ZFS components.

Dinse et al. observed that endohedral fullerene N@C_{60} in the ground state has a distorted structure when dissolved in a nematic phase.[10] Such a distortion is expected for pristine C_{60} as well; it also happens for other symmetric systems when embedded in the anisotropic environment of a nematic solvent.[21] If we assume that the distortion corresponds to an elongation along one C_5 axis as it occurs in the excited state by the Jahn−Teller effect, then C_{60} molecules will be preferentially oriented with one of these axes along the magnetic field just before the laser pulse excitation. We note that the last assumption means that C_{60} icosahedral geometry is most easily modified to D_{5d} symmetry independently of the source of the distortion.

The shape and polarization features of the TR-EPR spectra have been calculated using a dynamic model based on the fast exchange among sites[22] corresponding to differently oriented D_{5d} distorted structures. Experimental spectra corresponding to a long time delay were chosen for the fit to avoid the spectral

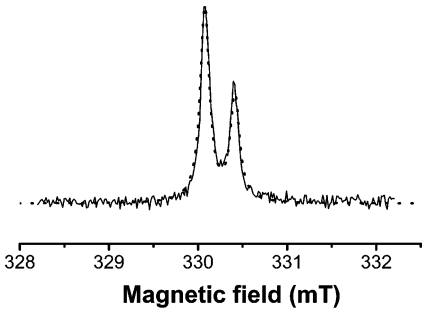

Figure 9. TR-EPR spectra of triplet C_{60} in E7 (nematic phase, T = 320 K) taken at a 15-μs delay time after the laser pulse (—) with the simulation described in the text (· · ·).

distortions due to fast relaxation at early times after the laser pulse excitation. (An example is reported in Figure 9.)

The six sites are distinguished by the orientation of their ZFS Z axis with respect to the magnetic field. Each site has a triplet spectrum consisting of two lines with a particular separation and polarization. In the nematic phase, the minimum energy of a C_{60} molecule elongated in the direction of a C_5 symmetry axis occurs when this axis coincides with the nematic director ($\theta = 0°$). This orientation, corresponding to a triplet line separation $\Delta(0°) = 2D$, was assumed to be one of the six sites together with other five sites that ensure that the ZFS anisotropy is averaged out as the order parameter tends to zero. In the latter five sites, which are equivalent to each other, the C_5 axis makes an angle of $\theta = 63.4°$ with the nematic director, and the triplet line separation is $\Delta(63.4) = -2D/5$. If $P(0)$ is the probability of finding C_{60} in site $\theta = 0°$, then the probability of sites $\theta = 63.4°$ is $P(63.4) = (1 - P(0))/5$. In the isotropic phase, $P(0) = P(63.4) = 1/6$, and in the nematic phase, $P(0) > 1/6 > P(63.4)$.

If fast jumping is considered among all six sites, then the resulting spectrum is characterized by the weighted average of the splitting and polarization corresponding to $\theta = 0$ and 63.4°. Of course if the environment is isotropic, then all of the sites are equally weighted (each one by $1/6$), and the splitting vanishes.

In the nematic phase, the observed splitting is accounted for by the probability of the $\theta = 0°$ site greater than $1/6$. An example of a calculated spectrum is reported in Figure 9 together with the experimental spectrum recorded at 320 K. For all spectra in the nematic temperature range, the best fit requires an exchange rate larger than 10^{11} s^{-1}. Under these conditions, the lines are Lorentzians, and the probability factor affects only their splitting, whereas the spin relaxation times influence the line width.

The values of the probability that agree with the observed splitting is reported in Figure 5 as function of the reduced temperature. It follows the trend of the order parameter S with temperature.

With the above assumptions, the polarization pattern is explained as well. Using eq 8 and assuming that $D < 0$, the low-field line corresponds to the $T_{-1} \leftrightarrow T_0$ transition and it should be in absorption, and the high-field line corresponding to the $T_0 \leftrightarrow T_1$ transition should be in emission, as experimentally found.

C_{70}. The spectrum recorded in toluene at $T = 290$ K consists of a single line whose width ($\Delta B = 1.27$ mT) is larger than that of $^3C_{60}$ at the same temperature ($\Delta B = 0.03$ mT).

The spectrum of $^3C_{70}$ recorded in the nematic phase of E7 at 320 K at a 0.4-μs delay is shown in Figure 8A. It is characteristic of a partially oriented collection of triplet molecules. The spectrum is similar to that reported in the literature for $^3C_{70}$ in isotropic frozen solution.[22,13] However, in our case the relative intensity of the inner and outer features is modified.

The different characteristics of $^3C_{60}$ and $^3C_{70}$ spectra arise from the different motional regime. For $^3C_{60}$, the narrow line in the isotropic phase in both toluene and E7 ($T > 333$ K) is accounted for by the fast reorientation of the ZFS tensor axes due to the dynamic JT effect.[3] In $^3C_{70}$, the dynamic JT effect rotates the x and y dipolar axes, but the z dipolar axes is affected only by the diffusive rotational dynamics.[13]

The spectrum taken at long delays show a single broad line in absorption (Figure 8B). A splitting in two components is not observed because of the large line width. An analysis of the orientation order similar to that performed for C_{60} is therefore not allowed.

Time Evolution. The time evolution of the TR-EPR signals of $^3C_{60}$ in the isotropic phase differs from that observed in the nematic phase. In the former case, the signal initially has zero intensity. It grows slowly, reaching a maximum about 2 μs after the laser pulse. This behavior was explained by assuming equal initial populations of the T_1 and T_{-1} Zeeman sublevels.[7] In fact, in the high-field approximation $B \gg D, E$, which is valid for the C_{60} triplet state, the intersystem crossing populating rates of the T_{-1} and T_1 triplet sublevels are the same, whatever the molecular orientation.

Because in the isotropic phase the two triplet transitions of $^3C_{60}$ are degenerate and have opposite polarization, the total EPR intensity due to the sum of the $T_{-1} \leftrightarrow T_0$ and $T_0 \leftrightarrow T_1$ transitions vanishes independently of the population of the T_0 sublevel. The increase in the TR-EPR signal is due to the buildup of magnetization caused by the spin−lattice relaxation, which brings the spin populations to thermal equilibrium.[23] The value of τ_1 reported in Table 1 is therefore an estimate of the spin−lattice relaxation time T_1 of $^3C_{60}$. After reaching thermal equilibrium, the signal decays with a characteristic time τ_2 that corresponds to the triplet lifetime.[8]

In the nematic phase where the $T_{-1} \leftrightarrow T_0$ and $T_0 \leftrightarrow T_1$ transitions are resolved into two components, the EPR signal increases very quickly to a maximum value in a period of time comparable with the spectrometer response time. The low-field transition in enhanced absorption decays as a double-exponential function. The initial fast decay rate is attributed to spin−lattice relaxation to thermal equilibrium; the second one is due to triplet decay to the electronic ground state. The triplet lifetime is not appreciably modified with respect to the value in the isotropic phase. The high-field transition initially in emission evolves quickly into absorption as spin−lattice relaxation brings the level populations toward thermal equilibrium. However, the Boltzmann equilibrium among the three levels is not completely reached. In fact, it would correspond to almost equal intensity of the two EPR lines,[24] which is not the case even at delay times much longer than the relaxation time (Figure 9).

Whereas the sum of the two TR-EPR signals reflects the population difference existing between T_1 and T_{-1}, their difference should give the population deviation from thermal equilibrium. If the polarization of the $T_{-1} \leftrightarrow T_0$ and $T_0 \leftrightarrow T_1$ transitions were the same though of opposite sign, then the above difference should decay fast to a vanishing value with the spin−lattice relaxation rate because at thermal equilibrium the population difference between T_0 and T_{-1} is practically the same as that between T_1 and T_0. Figure 10 shows that this is not the case because a residual signal remains at longer times. A nonvanishing intensity could arise if the $T_{\pm1}$ and T_0 triplet sublevels decay with different rates. The experimental data are fit by a kinetic model describing the time dependence of the spin sublevel populations.

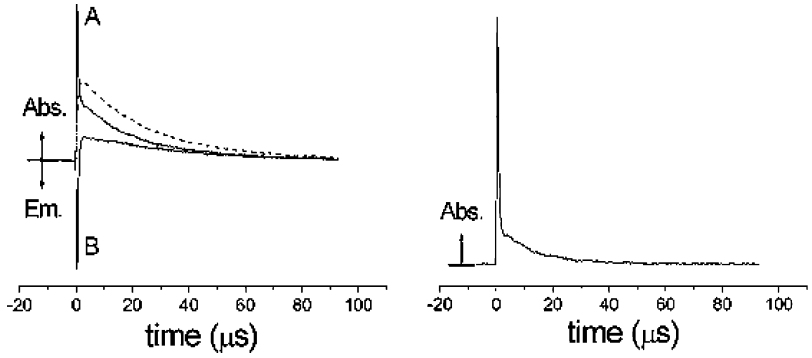

Figure 10. Time evolution of $^3C_{60}$ TR-EPR signals in the nematic phase of E7 ($T = 320$ K). (Left) low-field line (A) and high-field line (B) time signals and their sum (- - -). (Right) difference in the high- and low-field EPR signals.

According to this model, the triplet levels are connected by W_{ij}, the transition probability per unit time of the $j \leftarrow i$ transition. Each level decays with its own decay constant K_i. The kinetic equations of the sublevel populations N_{+1}, N_0, and N_{-1} are described in eqs 9:

$$\frac{dN_{+1}}{dt} = -K_{+1}\cdot N_{+1} - W_{+1,0}\cdot N_{+1} + W_{0,+1}\cdot N_0$$

$$\frac{dN_0}{dt} = -K_0\cdot N_0 - W_{0,-1}\cdot N_0 - W_{0,+1}\cdot N_0 + W_{+1,0}\cdot N_{+1} + W_{-1,0}\cdot N_{-1} \quad (9)$$

$$\frac{dN_{-1}}{dt} = -K_{-1}\cdot N_{-1} - W_{-1,0}\cdot N_{-1} + W_{0,-1}\cdot N_0$$

The microwave field effect on the populations is not considered because the transient signals were recorded using very low microwave power (100 μW). We have also verified that higher microwave power has no effect on the signal time evolution. The $\Delta m = 2$ relaxation is not included because its effect is negligible for the X band and at this temperature.[13] It is convenient to define a polarization parameter N_p:

$$(N_i - N_j)^{pol} = (N_i - N_j)^{eq}\cdot N_p \quad (10)$$

The subscripts pol and eq indicate, respectively, polarized states and thermal equilibrium states. In the absence of polarization, $N_p = 1$

The transition probabilities were calculated from the spin−lattice relaxation time T_1 measured in the isotropic phase (Table 1). The kinetic equations have been solved numerically by using the population rates as the initial values of the sublevel populations.

At T = 320 K, the experimental data are reproduced by the calculated data using the following set of parameters: N_p $(t = 0) = 15.0 \pm 0.5$; $1/K_{+1} = 23.0 \pm 0.5$ μs; $1/K_0 = 25.6 \pm 0.5$ μs; $1/K_{-1} = 25 \pm 0.5$ μs. It has to be noted that in order to fit the experimental data different decay rate constants of the single sublevels should be used.

Broad Signal Features. Concerning the quickly decaying broad signal of $^3C_{60}$ observed at low temperatures but still in the nematic-phase range from 265 to about 290 K, we note that it cannot be accounted for by the model that considers a quickly tumbling molecule in an anisotropic medium. The spectrum resembles that recorded in a glassy state, as, for example, in toluene at low temperatures, with some differences concerning the width and the polarization features. The same signals are observed if $^3C_{60}$ is dissolved in different nematic solvents, ruling out the possibility of an effect due to impurities in the solvent. (See Figure 6.)

We propose an explanation based on the presence of two phases in our sample, which should consists of ordered liquid-crystalline regions and regions where the nematic order is destroyed. We note that upon light absorption the C_{60} molecules undergoing ISC to the triplet state dissipate in the form of heat a large amount of energy corresponding to the singlet−triplet separation ($\Delta E_{ST} = 1600$ cm^{-1}). This energy is sufficient to destroy locally the nematic order in such a way that the molecule is located in a isotropic liquid at a temperature well below the nematic isotropic temperature. The local viscosity of the supercooled liquid is expected to be much higher than the viscosity of E7 at the temperature where the isotropic phase is stable. In such a situation, the EPR spectrum of the triplet C_{60} molecule corresponds to that of a random distribution of triplet excited molecules subjected to rotational diffusion in the slow-motion regime. The reorganization of the isotropic regions into nematic ordered ones causes the broad signal decay, which is much faster decaying than that or the narrow feature. The effect of energy dissipation on the local environment was also described by Terazima et al., who studied $^3C_{70}$ in frozen toluene.[25]

The presence of the excited triplet C_{60} in nematic regions (partially ordered $^3C_{60}$ giving rise to the narrow doublet of lines) is accounted for by its excitation through triplet−triplet energy transfer, which does not need energy release to the solvent.

Another explanation of the broad features could be the formation of C_{60} clusters or the existence of different phases. E7 is a mixture of compounds, and it is possible to have the coexistence of ordered and disordered phase. The disordered phase behaves as a viscous liquid, and the spectrum appears to be that of a random triplet molecule subjected to a slow-diffusion regime.

Conclusions

Triplet C_{60} in the nematic phase of liquid-crystal E7 shows two narrow EPR lines. Their separation and width are accounted for by pseudorotation among Jahn−Teller distorted structures. However, in contrast to what occurs in isotropic phases, pseudorotation does not involve isotropically distributed distorted structures. In the presence of a nematic potential, the energy is lowered for those distorted C_{60} molecules elongated in the direction of the liquid-crystal director. Additional features observed at low temperature in the nematic range are accounted for by the local destruction of nematic order due to energy dissipation in the intersystem crossing process. Triplet C_{70} is found to behave similarly to C_{60} derivatives whose low symmetry does not require pseudorotation involving the z axis

of the electron dipolar interaction tensor. The TR-EPR signal decay is described by a kinetic model that must include selective decay rates of the triplet sublevels.

Acknowledgment. This work was supported by MIUR (contract no. 2002032171). Helpful discussions with Professor A. Ferrarini and Professor A. Polimeno are gratefully acknowledged.

References and Notes

(1) Lane, P. A.; Swanson, L. S.; Ni, Q.-X.; Shinar, J.; Engel, J. P.; Barton, T. J.; Jones, L. *Phys. Rev. Lett.* **1992**, *68*, 887−890.

(2) Wasielewski, M. R.; O'Neil, M. P.; Lykke, K. R.; Pellin, M. J.; Gruen, D. M. *J. Am. Chem. Soc.* **1991**, *113*, 2774−2776.

(3) Closs, G. L.; Gautham, P.; Zhang, D.; Krusic, P. J.; Hill, S. A.; Wasserman, E. *J. Phys. Chem.* **1992**, *96*, 5228−5231.

(4) Zhang, D.; Norris, J. R.; Krusic, P. J.; Wasserman, E.; Chen, C.; Lieber, C. M. *J. Phys. Chem.* **1993**, *97*, 5886−5889.

(5) Regev, A.; Gamliel, D.; Meiklyar, V.; Michaeli, S.; Levanon, H. *J. Phys. Chem.* **1993**, *97*, 3671−3679.

(6) Steren, C. A.; van Willigen, H.; Dinse, K.-P. *J. Phys. Chem.* **1994**, *98*, 7464−7469.

(7) Agostini, G.; Corvaja, C.; Pasimeni, L. *Chem. Phys.* **1996**, *202*, 349−356.

(8) Goudsmit, G. H.; Paul, H. *Chem. Phys. Lett.* **1993**, *208*, 73−78.

(9) Groenen, E. J. J.; Poluektov, O. G.; Matsushita, M.; Schmidt, J.; van der Waals, J. H.; Meijer, G. *Chem. Phys. Lett.* **1992**, *197*, 314−318.

(10) Mayer, C.; Harneit, W.; Lips, K.; Weidinger, A.; Jakes, P.; Dinse, K.-P. *Phys. Rev. A* **2002**, *65*, 061201.

(11) Levanon, H.; Meiklyar, V.; Michaeli, S.; Gamliel, D. *J. Am. Chem. Soc.* **1993**, *115*, 8722−8727.

(12) Gamliel, D.; Levanon, H. *Stochastic Processes in Magnetic Resonance*; World Scientific: Singapore, 1995.

(13) Dauw, X. L. R.; Poluektov, O. G.; Warntjes, J. B. M.; Bronsveld, M. V.; Groenen, E. J. J. *J. Phys. Chem. A* **1998**, *102*, 3078−3082.

(14) Visser, J.; Groenen, E. J. J. *Chem. Phys. Lett.* **2002**, *356*, 43−48.

(15) Nordio, P. L.; Segre, U. In *The Molecular Physics of Liquid Crystals*; Luckhurst, G. R., Gray, G. W., Eds.; Academic Press: London, 1979.

(16) Ceola, S.; Corvaja, C.; Franco, L. *Mol. Cryst. Liq. Cryst.* **2003**, *394*, 31−43.

(17) Bennati, M.; Grupp, A.; Mehring, M. *J. Chem. Phys.* **1995**, *102*, 9457−9464.

(18) Actually, the EPR spectrum recorded at very low temperature corresponds to lower symmetry, lacking an axis of order $n \geq 3$ because the ZFS parameter E does not vanish. A rhombic distortion starting from D_{5d} symmetry is compatible with this observation.

(19) Gamliel, D.; Levanon, H. *J. Chem. Phys.* **1992**, *97*, 7140−7159.

(20) Surján, P. R.; Németh, K.; Bennati M.; Grupp, A.; Mehring, M. *Chem. Phys. Lett.* **1996**, *251*, 115−118.

(21) *NMR of Ordered Liquids*; Burnell, E. E.; de Lange, C. A., Eds.; Kluwer: Dordrecht, The Netherlands, 2003.

(22) Sullivan, P. D.; Bolton, J. R., *Adv. Magn. Reson.* **1965**, *1*, 39−85.

(23) Careful measurements made by FT-EPR (see ref 6) showed that the initial spin polarization is actually 0.2 times the Boltzmann equilibrium value.

(24) At temperatures close to 300 K and at the magnetic field of $B \approx$ 300 mT used in the X-band spectrometer, the expected intensity difference of the $T_{-1} \leftrightarrow T_0$ and $T_0 \leftrightarrow T_1$ transitions is only 0.1%.

(25) Terazima, M.; Sakurada, K.; Hirota, N.; Shinobara, H.; Saito, Y. *J. Phys. Chem.* **1993**, *97*, 5447−5450.